HHS Public Access

Author manuscript

*Nat Neurosci*. Author manuscript; available in PMC 2010 September 01.

Published in final edited form as:

*Nat Neurosci*. 2010 March ; 13(3): 327–332. doi:10.1038/nn.2487.

# Disrupted-in-Schizophrenia-1 (DISC1) regulates spines of the glutamate synapse via Rac1

**Akiko Hayashi-Takagi**[1], **Manabu Takaki**[1], **Nick Graziane**[2], **Saurav Seshadri**[1], **Hannah Murdoch**[3], **Allan J Dunlop**[3], **Yuichi Makino**[4], **Anupamaa J Seshadri**[1], **Koko Ishizuka**[1], **Deepak P. Srivastava**[5], **Zhong Xie**[5], **Jay M. Baraban**[4], **Miles D. Houslay**[3], **Toshifumi Tomoda**[6], **Nicholas J. Brandon**[7], **Atsushi Kamiya**[1], **Zhen Yan**[2], **Peter Penzes**[5], and **Akira Sawa**[1,4]

[1] Dept of Psychiatry, Johns Hopkins University School of Medicine, Baltimore, MD

[2] Department of Physiology and Biophysics, University at Buffalo, SUNY

[3] Division of Biochemistry and Molecular Biology, Institute of Biomedical and Life Sciences, University of Glasgow

[4] Dept of Neuroscience, Johns Hopkins University School of Medicine, Baltimore, MD

[5] Department of Physiology, Northwestern University Feinberg School of Medicine

[6] Beckman Research Institute of the City of Hope

[7] Pfizer, Princeton, NJ

## Abstract

Synaptic spines are dynamic structures that regulate neuronal responsiveness and plasticity. Here we describe a role for the schizophrenia risk factor, Disrupted-in-Schizophrenia 1 (DISC1), in the maintenance of spine morphology and function. We show that DISC1 anchors Kalirin-7 (Kal-7) thereby regulating access of Kal-7 to Rac1 and so controlling the duration and intensity of Rac1 activation in response to NMDA receptor activation in cortical culture as well as *in vivo* brain. This offers explanation for why Rac1 and its activator (Kal-7) serve as key mediators of spine enlargement and that constitutive Rac1 activation decreases spine size. This novel mechanism likely underlies disturbances in glutamatergic neurotransmission frequently reported in schizophrenia that can lead to alteration of dendritic spines with consequential major pathological changes in brain function. Furthermore, the concept of a “signalosome” involving disease-associated factors, such as DISC1 and glutamate, may well contribute to the multifactorial and polygenetic characteristics of schizophrenia.



Correspondence and requests for materials should be addressed A.S. (asawa1@jhmi.edu).

**AUTHOR CONTRIBUTIONS**

A.H-T., M.T., N.G., S.S., H.M., A.J.D., and T.T. conducted experiments. Y.M., A.J.S., K.I., D.P.S., Z.X. conducted critical scientific assistance for experiments. J.M.B., M.D.H., T.T., N.J.B., A.K., Z.Y., P.P. contributed intellectual and scientific contributions to carry out experiments. A.H-T. M.D.H., T.T., N.J.B., and A.S. wrote the manuscript. A.S. led the overall experimental design of the entire project.

Disturbances in neuronal connectivity, especially glutamatergic synaptic connections, underlie schizophrenia and associated disorders[1–3]. Neuropathological studies with autopsied brains from patients with schizophrenia have reported reduced numbers of dendritic spines[4, 5]. Morphological changes of the dendritic spine are directly correlated with its functional deficits[6, 7]. Indeed, in brains of patients with schizophrenia, alteration of levels of glutamate and its metabolite *N*-acetylaspartate levels is detected by magnetic resonance spectroscopy[8]. Furthermore, some studies suggest a reduction in glutamate receptor binding in the prefrontal cortex of individuals with schizophrenia using a selective tracer for the NMDA receptor [$^{123}$I] CNS-1261 in single photon emission tomography[9]. Consistent with these findings, molecular profiling studies on postmortem brain from patients with schizophrenia indicate decreases in key synaptic molecules[10]. These include Kal-7 and Rho-family small G-proteins[11], which play crucial roles in spine structural and functional plasticity[12, 13]. This notion has been reinforced by the recent discovery of genetic susceptibility factors for schizophrenia that are enriched in the dendritic spine, including Neuregulin-1, ErbB4, RGS4, and CAPON[14, 15], some of which reportedly interact with PSD95, a major structural protein of the postsynaptic density of the glutamate synapse[16, 17].

DISC1 is another promising susceptibility factor for schizophrenia and related disorders, and its disruption due to balanced chromosomal translocation results in a familial psychosis in a large Scottish pedigree[18]. Importantly, several studies have reported that common variants of DISC1 are associated with endophenotypes relevant to schizophrenia, including decreased gray matter volume and poor working memory[19–22]. By conducting immunoelectron microscopy, we have previously reported that a pool of DISC1 is enriched in the postsynaptic density in human brains[23]. Morphological changes of spines have been reported in an animal model in which some DISC1 isoforms are genetically deleted[24]. Here we describe a novel and crucial mechanism that shows how DISC1 regulates synaptic spines, whereby DISC1 anchors Kal-7 in a protein complex and limits and controls access of Kal-7 to Rac1 in response to activation of the NMDA glutamate receptor.

## RESULTS

### DISC1 modulates morphology and function of synaptic spines

Consistent with our histological data with human brains, we observed enrichment of DISC1 in the Triton X-100-resistant postsynaptic density (PSD) fractions of adult rat brains (Supplementary Fig. 1a). Synaptic DISC1 becomes prominent in mature neurons, whereas centrosomal DISC1, evident in proliferating cells and immature neurons, disappears (Supplementary Fig. 1b). To test possible roles for DISC1 in the PSD of mature neurons, RNA interference (RNAi) was utilized[25]. Two independent short-hairpin RNAs (shRNAs) knocked down both HA-tagged full-length exogenous DISC1 (DISC1-FL) and major isoforms of endogenous DISC1 (Supplementary Fig. 2). Application of DISC1 RNAi resulted in a decrease of DISC1 in postsynaptic spines (Supplementary Fig. 3), resulting in increased size and number of spine-like structures 2 days after DISC1 RNAi application (Fig. 1a, Supplementary Fig. 4). These spine-like structures likely formed functional synapses, as indicated by increases in the surface expression of the AMPA-type glutamate receptor GluR1 (Fig. 1b, Supplementary Fig. 5), a key mechanism of synaptic

potentiation[26]. Increased frequency of miniature excitatory postsynaptic currents (mEPSC) in neurons with DISC1 knockdown was observed electrophysiologically (Fig. 1c). To rule out the possibility of "off-target" effects of RNAi, we carried out quantitative real-time PCR for 2′, 5′-oligoadenylate synthetase (OAS1). No induction of OAS1 was observed with control and DISC1 RNAi (Supplementary Fig. 2d). These data indicate a regulatory role for DISC1 in spines.

## Binding of DISC1 with Kal-7 is crucial for its modulation of spines

DISC1 interacts with many proteins, including several synaptic proteins[21, 22]. Among these synaptic proteins, identified as putative DISC1 partners by yeast two-hybrid screenings, Kal-7, a GDP/GTP exchange factor (GEF) for Rac1, is well known as a regulator of spine morphology and plasticity in association with neuronal activity[27]. Indeed, recent studies demonstrated that Kal-7 is required for proper spine formation[28, 29]. Like other proteins associated with schizophrenia, Kal-7 interacts with PSD95 (ref. [27]). Thus, we hypothesized that DISC1 might regulate Kal-7 in conjunction with PSD95. Interaction of Kal-7 and PSD95 with DISC1 was confirmed by co-immunoprecipitation from primary cortical neurons and rat brains, especially in the synaptosome (Fig. 2a). In contrast, DISC1 did not interact with other GEFs[30, 31], such as Tiam-1 and βPIX (Fig. 2a). To ascertain the domain of DISC1 critical for binding Kal-7, we first examined a variety of deletion constructs of DISC1. This showed that deletion of amino acids 350–394 of DISC1 (DISC1-ΔKal-7) abolished DISC1/Kal-7 binding (Supplementary Fig. 6a). This is in agreement with yeast two-hybrid screening in which N-terminal DISC1 (amino acids 1–382) interacted with a fragment of Kal-7 (Supplementary Fig. 6a, b). The binding domain(s) of DISC1 for Kal-7 were further validated by peptide array analysis, which relies on direct protein-peptide interactions[32]. Here a scanning library of 25-mer peptides, each displaced in sequence by 5 amino acids and reflecting the entire sequence of DISC1, was probed with a purified recombinant Kal-7 fragment (amino acids 588–1137), which corresponds to the domain for DISC1 binding that was identified by co-immunoprecipitation with various deletion mutants of Kal-7 (Supplementary Fig. 6b, c). Peptides that contained amino acids 376–405 of DISC1 showed the strongest interaction signal with recombinant Kal-7, in agreement with the data from deletion mutants and the notion that DISC1 interacts directly with Kal-7 (Supplementary Fig. 6c). The Kal-7 binding domain on DISC1 (amino acids 350–394) is distinct from that required for interaction with cAMP phosphodiesterase-4 (PDE4) or the kinesin superfamily member KIF5 (ref. [33–35]) (Supplementary Fig. 6d, e). Overexpression of DISC1-FL decreased spine size in neurons 2 days after transfection, whereas DISC1-ΔKal-7 did not (Fig. 2b, Supplementary Fig. 7). This result is consistent with the increased spine size seen upon knockdown of DISC1 (Fig. 1a). Moreover, DISC1 RNAi-induced spine enlargement and increase in mEPSC frequency were completely normalized by the overexpression of DISC1-FL$^{R}$ (the equivalent to DISC1-FL at the amino acid level, but 3 nucleotide mutations at the nucleotide levels of its expression construct), but not by that of DISC1-ΔKal-7$^{R}$ (Fig. 2c, d). Knockdown of DISC1 did not, however, affect the localization of Kal-7 in the spines (Supplementary Fig. 8). These results support the notion that DISC1/Kal-7 protein interaction in the spine is crucial for regulating its morphology.

### Influence of NMDAR on DISC1/Kal-7/PSD95/Rac1 signaling

We next addressed the molecular mechanism by which DISC1 affects Kal-7 activity and subsequently spine morphology. Since Kal-7 binds to PSD95 (ref. [27]), we tested whether DISC1 might influence the interaction of these two proteins. In primary neurons overexpression of DISC1-FL markedly increased the binding between Kal-7 and PSD95, while overexpression of the deletion construct, DISC1-ΔKal-7, did not (Fig. 3a). In contrast, knockdown of DISC1 reduced the Kal-7/PSD95 interaction in primary cortical neuron cultures (Fig. 3b, Supplementary Fig 9a). These results suggest that DISC1 functions as a molecular signaling scaffold that augments Kal-7/PSD95 interaction.

The signaling of Kal-7 to Rac1 is coupled with neuronal activity via the NMDA receptor[27]. Therefore, we examined how neuronal activity might modulate protein interactions among Kal-7, PSD95, and DISC1 by utilizing electroconvulsive treatment (ECT), which elicits neuronal activation *in vivo*[36]. We observed significant decreases in protein interactions between Kal-7/PSD95, Kal-7/DISC1, and DISC1/PSD95 in brain homogenates after ECT (Fig. 4a, Supplementary Fig 9b). To confirm that these changes were due to neuronal activation via the NMDA receptor in primary neurons, we used an established protocol in which withdrawal of amino-5-phosphonovaleric acid (APV), a potent inhibitor of the NMDA receptor, is utilized to activate the receptor[27]. Dissociation of the DISC1/Kal-7/PSD95 complex was observed upon APV withdrawal (APV WD), suggesting that the altered protein-protein interactions were dependent on activation of the NMDA receptor (Fig. 4b, Supplementary Fig 9c). Activation of Rac1 was also observed upon APV withdrawal (Fig. 4b). These findings suggest that Kal-7 is released from DISC1 in an activity-dependent manner where the resultant free Kal-7 might activate Rac1, and thereby modulating spine structure.

To validate this notion, we assessed whether Rac1 activation could be influenced by DISC1. Activation of Rac1, determined by the level of GTP-bound Rac1, was significantly reduced by transfection of DISC1-FL, but not by DISC1-ΔKal-7, in primary neurons (Fig. 5a). Accordingly, DISC1 knockdown led to Rac1 activation, detected by increased GTP-bound Rac1 and phosphorylation of p21-activated kinase (Pak1) (Fig. 5a). Furthermore, decrease in Rac1/Kal-7 binding was observed when DISC1-FL was overexpressed (Fig. 5b). This blockade was significantly reduced when DISC1-ΔKal-7 was expressed in neurons. These results are consistent with the notion that DISC1 blocks Rac1 activation by inhibiting access of Kal-7 to Rac1. Stoichiometric analyses with recombinant DISC1, Kal-7, and PSD95 indicated that DISC1, as a scaffold protein, could efficiently anchor Kal-7 and PSD95 (Supplementary Figs. 10 and 11). This observation is consistent with the nature of these proteins to be prone to oligomerize[37, 38]. In accordance with previous reports[39], we confirmed that Kal-7 selectively activates Rac1, but not Cdc42 and RhoA (Supplementary Fig 12). The presence of a functional DISC1/Kal-7/Rac1 ‘signalosome’ is also supported by the findings that DISC1 RNAi-induced spine enlargement was abolished by co-transfection with either Kal-7 RNAi (data not shown) or a dominant-negative (DN) Rac1 construct (Fig. 5c, Supplementary Fig. 13). Together these data imply that Kal-7 is anchored to PSD95 via DISC1 and that this complex is modulated dynamically by neuronal activation, providing a key regulatory step for Rac1-mediated spine morphology.

### Long-term effects of DISC1 on dendritic spines

Although activation of Rac1 initially leads to rapid spine growth, prolonged activation of Rac1 results in spine shrinkage in brains[40, 41]. Thus, we examined this paradoxical action of Rac1 on spine morphology in our neuron cultures by introducing a constitutively-active Rac1 (Rac1-CA) construct. One day after transfection, we observed transient overgrowth of spines in neurons expressing Rac1-CA, compared with neurons expressing either wild-type Rac1 or Rac1-DN. In contrast, 6 days after transfection, the spine size in neurons with Rac1-CA became even smaller than those in neurons expressing wild-type Rac1 or Rac1-DN (Fig. 6a). This result is consistent with the notion that, although Rac1 activation is crucial for rapid spine growth, its continuous activation leads to deleterious effects on spines. As DISC1 may control access of Kal-7 to Rac1, we tested whether modulation of DISC1 results in similar time-dependent effects on spines. Knockdown of DISC1 might be expected to increase continuous access of Kal-7 to Rac1, leading to a condition similar to that seen upon the introduction of Rac1-CA, whereas overexpression of DISC1 might be expected to decrease access of Kal-7 to Rac1, a condition similar to that resulting from Rac1-DN or Kal-7 knockdown. Knockdown effects of DISC1 RNAi by plasmid vector can last for at least 6 days (Supplementary Fig. 2b). As predicted, we observed that the prolonged DISC1 knockdown, which was associated with decreased PSD95/Kal-7 binding and increased Rac1 activity (Supplementary Fig. 14), markedly reduced spine size in primary cortical neurons (Fig. 6b, c). Overexpression of DISC1 also resulted in reduced spine size 6 days after transfection (Fig. 6b). These small spines induced by continuous knockdown of DISC1 showed decreased surface expression of GluR1 and reduced frequency of mEPSC, suggesting that structural shrinkage of spines was accompanied by a functional alteration (Fig. 6d). Spine deterioration by prolonged DISC1 suppression was significantly rescued by overexpression of DISC1-FL$^{R}$, but not by that of the mutant DISC1-ΔKal-7$^{R}$ (Fig. 6e, **f**). To test long-term effects of DISC1 suppression in brain circuitry, we first used organotypic cortical cultures. Introduction of lentivirus-based shRNA to DISC1 for 7 days resulted in smaller spines in pyramidal neurons of cortical organotypic culture (Fig. 7a). Furthermore, robust shrinkage of synaptic spine was observed when shRNA to DISC1 was stereotaxically introduced into the medial prefrontal cortex of juvenile rats (Fig. 7b).

## DISCUSSION

This study provides novel functional and structural insight into the role of DISC1 in dendritic spines, where DISC1 regulates Rac1 activation by confining access of Kal-7 to Rac1 (see Supplementary Fig. 16 for a scheme). Although the Kal-7/Rac1 cascade was known to be a key determinant of neuronal activity-dependent spine morphological and functional plasticity[27], the mechanism underlying its regulation was not clear. Our study provides a new concept where the “schizophrenia-related” protein, DISC1 plays a key role in mediating proper synaptic maintenance associated with neuronal activity, by being closely coupled with the activation of the NMDA receptor and limiting the access of Kal-7 to Rac1 in the PSD scaffold.

DISC1 potentially binds with proteins other than Kal-7 in the synaptic spines, such as PDE4B and KIF5 (ref. [21, 22, 42]) (Supplementary Fig. 6d, e). Nonetheless, the present data

support the notion of spine regulation by DISC1/Kal-7/Rac1 in association with PSD95, without direct involvement of DISC1/PDE4B and DISC1/KIF5 protein cascades. It is possible that other genetic risk factors for schizophrenia that are known to interact with PSD95, such as CAPON and ErbB4 (ref. [15]), might indirectly modulate this proposed cascade for spine regulation. DISC1 is known to have many isoforms[43]. Our data, especially those of rescue experiments with DISC1-FL$^R$ indicate that the full-length isoform of DISC1 plays a major role in the Kal-7/Rac1 cascade by forming a DISC1/Kal-7/Rac1 signalosome whose function is spatially restricted and likely focused on outputs governed by the NMDA receptor action.

Schizophrenia is believed to be associated with disturbance of neuronal connectivity[2], [3]. Many epidemiological studies have indicated that initial and major risks for the disease occur during neurodevelopment, although onset of the disease occurs in juveniles and young adulthood[44]. Therefore, it is important to address mechanisms that can contribute to the onset of the disorders. Deficits in postnatal synaptic pruning at glutamate synapses that occur just prior to the onset are hypothesized as a potential mechanism[45]. The expression of full-length DISC1 reaches a peak at postnatal day 35 (ref. [46]) when synaptic pruning is actively taken place[47]. It is, therefore, possible that disturbances in the DISC1/Kal-7/Rac1 signalosome-mediated synaptic maintenance may contribute to the juvenile onset of the diseases. Recent clinical studies have focused on subjects in the prodromal stages of schizophrenia and are exploring preventive medications that can block the progression of pre-psychotic conditions to full disease onset[48]. Thus, this disease etiology-associated molecular pathway we propose through the DISC1/Kal-7/Rac1 signalosome may help in identifying such therapeutic strategies that selectively target subjects with specific genetic risks.

## METHODS

### Antibodies

N-terminal polyclonal antibody against DISC1 was a generous gift from Dr Gogos (Columbia univ.)[49]. Additional DISC1, Kal-7 specific, and Kal-spectrin antibodies were previously described[25], [27]. Antibodies to myc (Santa Cruz Biotechnology, Santa Cruz, CA), PSD95 (NeuroMab, Davis, CA), synaptophysin (Sigma-Aldrich Corp, St. Louis, MO), KIF5 (Millipore, Bedford, MA), GFP (Invitrogen, Eugene, OR), HA(Covances), phospho-Pak1 (Cell Signaling technology, Danvers, MA), Pak1 (Cell Signaling technology), Tiam1 (Santa Cruz), GluR1(Millipore), βPIX (Millipore), andAlexa 405-, 488-, 568- or 633-conjugated secondary antibodies (Invitrogen) were used.

### Plasmid construction and transfection

Cloning, mutagenesis, and deletion of DISC1 and Kal-7 were conducted as described in the prior publication[25]. Wild-type, constitutively-active (Rac1-CA, G12V), and dominant-negative form of Rac1 (Rac1-DN, T17N) were from Missouri University of Science and Technology (Rolla, MO). H1-RNA polymerase III promoter-driven shRNA against DISC1 (#1 with strong effect and #2 with weaker effect), which also carry EGFP under the downstream of CMV promoter, were previously described[25]. Cultured cells were transfected

with plasmids by the use of LipofectAMINE2000 (Invitrogen). In primary neuron culture, 2μg of pSuper-Venus RNAi were transfected into $1.5 \times 10^5$ cells. For 293 cells, 2 μg of pRK/DISC1-HA expression construct and 2 μg of pSuper-Venus RNAi construct were transfected (at 90 % confluence in 18 mm dish). In standard analyses, primary neurons were transfected after 23 DIV and maintained for 1–6 days after transfection.

### Recombinant proteins tagged with GST or MBP

The full-length mouse DISC1 cDNA was cloned in pMAL vector for DISC1-MBP. Likewise, the full-length PSD95 and Kal-7 (amino acid 588–1571) were cloned in pGEX for PSD95-GST and Kal-7-GST, respectively. The expression plasmids were introduced into *E. coli* BL21, grown at 23 °C with 0.1 mM IPTG. Recombinant proteins were purified from *E. coli* with glutathione sepharose or amylose beads. Further purification was conducted with a centrifugal filter device, Amicon Ultra-100k (Millipore), by which degraded protein fragments at less than 100 kDa were removed.

### Viral production and infection

Lentivirus was produced by co-transfection of RNAi-containing FUGW lentiviral constructs and helper constructs VSVG and Δ8.9 into 293FT packaging cells. Media were collected 48 h after transfection and virus was concentrated by ultracentrifugation at 25,000 × g for 90 min. For synthesis of Sindbis virus, recombinant RNAs from Sindbis vector pSinRep5 (nsP2) and packaging construct DH(26)S were generated by *in vitro* transcription with use of the mMESSAGE mMACHINE kit (Ambion). These RNAs were transferred into BHK cells with GenePulser XCell system (BioRad), followed by collection of media after 24 h. Viral titers were calculated by counting EGFP-positive cells after infecting with serial dilutions of the viral solution. For infection into a primary neuron, virus solution was added to the medium ($3.5 \times 10^5$ unit/$1.5 \times 10^5$ cells), which was changed 24 h after infection, followed by incubation for 3–7 days to allow gene knockdown. For infection of slice cultures, 1 μl of $1.8 \times 10^5$ unit/μl solution was added directly to the slice. The morphology of infected cells was depicted by the fluorescence of EGFP carried in the viral vector.

### Neuron cultures and treatment

All procedures related to animals were performed according to the Johns Hopkins animal care and use guidelines. Dissociated cortical neuron cultures from Sprague-Dawley (SD) rat were prepared as described previously[25]. Withdrawal of DL-aminophosphonovalerate (APV) (Ascent Scientific, Weston-super-Mare, UK) was used for chemical activation of NMDA receptor. Briefly, 200 μM APV was added to the culture dish 5 days after plating, and was maintained in the medium with APV. For treatment of APV withdrawal, cells were preincubated in artificial cerebrospinal fluid (ACSF) (in mM: 125 NaCl, 2.5 KCl, 26.2 $NaHCO_3$, 1 $NaH_2PO_4$, 11 glucose, 5 HEPES, 2.5 $CaCl_2$, and 1.25 $MgCl_2$) with 200 μM APV for 30 min at 37°C. Coverslips were then washed in withdrawal medium (ACSF plus 30 μM *D*-serine, 100 μM picrotoxin, and 1 μM strychnine) and transferred into new withdrawal medium for 20 min. Cells were then immediately fixed for immunofluorescence or lysed with lysis buffer for biochemical analysis such as Rac1 assay and co-immunoprecipitation (see below). Organotypic cortical culture was prepared from cerebral

cortex of postnatal day 3 (P3) pups by using a McIlwain-type tissue chopper. A slice (400 μm thickness) was maintained on the Organotypic cell culture insert (Millipore), which are porous and transparent membranes, with neurobasal-N1 medium [Neurobasal medium (Invitrogen) supplemented with 2 mM L-glutamine, 5% horse serum, and N1 supplement (Sigma)].

## Electrophysiological Recordings

Recording for miniature excitatory postsynaptic currents (mEPSC) in cultured neurons ($n$ = 6 to 12 in each group) were prepared as described previously[50]. Patch electrodes (3–5 MΩ) were filled with the following internal solution [(130 mM Cs-methanesulfate, 10 mM CsCl, 4 mM NaCl, 1 mM $MgCl_2$, 5 mM EGTA, 10 mM HEPES, 5 mM MgATP, 0.5 mM $Na_2GTP$, 12 mM phosphocreatine, 20 mM leupeptin, and 1 mM QX314), pH 7.2–7.3, 265–270 mosm/l]. The external solution [127 mM NaCl, 5 mM KCl, 2 mM $MgCl_2$, 2 mM $CaCl_2$, 12 mM glucose, 10 mM HEPES, and 0.5 mM TTX), pH 7.4, 300 mosm/l]. Bicuculline (10 μM) was added to the external solution to block $GABA_A$ receptors. Recordings were obtained with an Axon Instruments 200B patch clamp amplifier that was controlled and monitored with an IBM PC running pCLAMP with a DigiData 1320 series interface (Axon instruments, Foster City, CA). Electrode resistances in the bath was typically 2–4 MΩ. After seal rupture, series resistance (4–10 MΩ) was compensated (70–90%) and periodically monitored. The cell membrane potential was held at −70 mV. The Mini Analysis Program (Synaptosoft, Leonia, NJ) was used to analyze synaptic activity. For each different condition, mEPSC recordings of 8 min were used for analysis.

## Immunofluorescence cell staining

Cells were fixed with 4% formaldehyde for 30 min at room temperature (RT). Experimental details for cell staining were as described previously[25]. For staining of surface GluR1 on the plasma membrane, fixed cells were incubated with a primary antibody against an extracellular region of GluR1, prior to permeabilization with Perm/Blocking buffer (2.5 % normal goat serum in PBS with 0.1 % Triton X-100). Then, permeabilized cells were stained for synaptophysin with the protocol for cell staining. For free-floating immunofluorescence staining of organotypic slice, the slices were fixed with 4% formaldehyde for 1 h at RT, followed by permeabilization with Perm/Blocking buffer (2.5 % normal goat serum in PBS with 0.3 % Triton X-100) for 1 h at RT. The slices were incubated for 48 h at 4°C with a primary antibody in Perm/Blocking buffer. After rinsing with PBS (8 times, 5 min each), sections were stained with corresponding secondary antibody, followed by mounting. Cell staining was examined with a confocal microscope (LSM 510-Meta, Zeiss, Minneapolis, MN).

## Quantitative morphological analysis of spine

Staining with anti-GFP antibody was used to circumvent potential unevenness of GFP diffusion in spines. For co-transfection experiments, the neurons that were clearly transfected with both GFP and gene of interest were captured as images. Images were taken by a Zeiss LSM510-Meta with the 63 x oil-immersion objective as z-series of 6 to 12 images taken at 0.3-μm intervals (scan averaged, four times; 1024 × 1024 pixel resolution; a scan

speed of 1.6 ms/pixel). The acquisition parameters were kept the same for all scans in the same experiment. Only first dendrites that were arborized from a typical apical dendrite of the authentic pyramidal neuron with triangle cell body were subjected to morphological analysis according to a protocol previously described[27]. Two-dimensional projection reconstructions of z-series of images, morphometric analysis, and quantification were done using MetaMorph software version 7.1 (MDS Analytical Technologies, Sunnyvale, CA). Individual spines on dendrites were manually traced, and the area (Size), maximum length (Length), and head width (Breadth) of each spine was measured. Based on the sensitivity of this quantitative morphological analysis, which has been already established[27], we did not consider structures that had an area of less than 0.25 $\mu m^2$ as the spine, because these are approaching the limit of resolution of our microscope. In each experiment, about 500 to 1000 spines from 30 to 45 dendrites derived from 10 to 15 neurons were analyzed per condition. At least two independent analyses, mostly three, were carried out while blinded to transfection condition until statistical analysis had been done.

### Preparation of synaptosomes and postsynaptic densities

Cerebral cortex dissected from adult SD rat was homogenized in 10 volumes of buffer A (0.32 M sucrose, 1 mM $NaHCO_3$, 1mM $MgCl_2$, and 0.5 mM $CaCl_2$). Crude synaptosomal and postsynaptic densities were purified using the classical sucrose gradient protocol previously described[27].

### Immunoprecipitation

Cells or tissue were lysed in lysis buffer [150 mM NaCl, 50 mM Tris·HCl, pH 7.4, 0.1% NP-40, and protein inhibitor cocktail (Complete; Roche Diagnostics, Indianapolis, IN)]. Lysates were sonicated, cell debris was cleared by centrifugation, and the soluble fraction was subjected to immunoprecipitation (IP), followed by immunoblotting (IB). Normal IgG (IgG) or Myc antibody was used as negative control for immunoprecipitation. The signal intensity of each band (the net signal is after subtraction of background signal obtained from the region adjacent to the band) was measured by ImageJ software (NIH, MD).

### Rac activation assay

Activation of Rac1 was measured with the Rac1 activity assay kit (Upstate Biotechnology, Waltham, MA) according to manufacturer's instructions. Briefly, fusion-protein corresponding to the p21-binding domain of Pak1, which specifically binds to the active form of Rac1 (Rac-GTP) but not to the inactive form of Rac1 (Rac-GDP), is used for precipitation for Rac-GTP. GTP-γs and GDP were used for positive and negative control for assay, respectively. Phosphorylation of Pak1, a substrate for Rac1, was also used as an indicator for Rac1 activity because the binding of Rac1-GTP to Pak1 causes autophosphorylation and activation of Pak1.

### Intracerebral injections of lentiviral vectors

SD rats, aged at P21–24, were anesthetized with ketamine and xylazine and placed in a stereotaxic frame to secure the cranium. An incision was made in the scalp and a hole was drilled in the skull at the desired site of injection. The location of the injection site in the

prefrontal cortex (PFC) was standardized among animals by using stereotaxic coordinates (AP = +2.2; ML = +1.0; DV = +1.0) from the skull. A total of 8 rats (4 for DISC1 RNAi, 4 for scrambled RNAi) were bilaterally injected with 3 μl of the lentiviral preparations ($1.8 \times 10^5$ unit/μl) into the medial prefrontal cortex (by using a Hamilton syringe, 0.15μl/min). Eight days after injection, rats were euthanized, and the brains were perfusion-fixed in 4% paraformaldehyde for subsequent immunohistochemical analysis. The morphology of infected cells was depicted by the fluorescence of EGFP carried in the viral vector. All procedures related to animals were performed according to the Johns Hopkins animal care and use guidelines.

### Electroconvulsive treatment (ECT)

ECT were induced in an unanesthetized SD rat at P21 by delivering AC current (Current, 90 mA; Frequency, 100 Hz; Pulse width, 0.5 ms; Shock duration, 1.0 s) via ear clip electrodes as described[36]. For biochemical analysis, animals were euthanized by cervical fracture, followed by dissection of cerebral cortex 3 min after electroconvulsion.

### Statistics

For determination of the statistical significance between two groups, either the Student's t-test (equal variances) or Mann Whitney U-tests (unequal variances) were employed. The result of the F-test was used to decide which test was appropriate. To compare three or more groups, one-way ANOVAs were used, followed by Dunnett-T3 post hoc for multiple comparisons. Statistical analyses were performed using SPSS 11.0 software (*$P < 0.05$; †$P < 0.01$; #$P < 0.001$). Error bar indicates s.e.m. Cross bar across a scattered plot indicates the mean of all values.

## Supplementary Material

Refer to Web version on PubMed Central for supplementary material.

## Acknowledgments

We thank Ms. Y. Lema and Dr. P. Talalay for manuscript preparation. We appreciate Drs. A. Gruber, P. O'Donnell, P.F. Worley, R.L. Huganir, J.D. Rothstein, N. Shahani, H. Ujike, S. Kuroda, H. Bito, and M. Nuriya for scientific discussions. We thank Drs. J. Gogos, R.A. Cerione, H. Cline, and Jeromin, A. for providing us with reagents. This work was supported by MH-084018 (A.S.), MH-069853 (A.S.), MH-088753 (A.S.), MH-071316 (P.P.), MH-084233 (Z.Y), and NS-048911 (Z.Y.) as well as grants from Stanley (A.S.), CHDI (A.S.), HighQ (A.S.), S-R (A.S.), RUSK (A.S.), NARSAD (A.S., A.H-T., A.K., and P.P), NAAR (P.P.), Uehara (A.H-T., M.T.), MRC G0600765 (M.D.H), and the European Union grant LSHB-CT-2006-037189 (M.D.H).

## References

1. Goff DC, Coyle JT. The emerging role of glutamate in the pathophysiology and treatment of schizophrenia. Am J Psychiatry. 2001; 158:1367–1377. [PubMed: 11532718]
2. Moghaddam B. Bringing order to the glutamate chaos in schizophrenia. Neuron. 2003; 40:881–884. [PubMed: 14659087]
3. McCullumsmith RE, Clinton SM, Meador-Woodruff JH. Schizophrenia as a disorder of neuroplasticity. Int Rev Neurobiol. 2004; 59:19–45. [PubMed: 15006483]
4. Glantz LA, Lewis DA. Decreased dendritic spine density on prefrontal cortical pyramidal neurons in schizophrenia. Arch Gen Psychiatry. 2000; 57:65–73. [PubMed: 10632234]

5. Garey LJ, et al. Reduced dendritic spine density on cerebral cortical pyramidal neurons in schizophrenia. J Neurol Neurosurg Psychiatry. 1998; 65:446–453. [PubMed: 9771764]
6. Maletic-Savatic M, Malinow R, Svoboda K. Rapid dendritic morphogenesis in CA1 hippocampal dendrites induced by synaptic activity. Science. 1999; 283:1923–1927. [PubMed: 10082466]
7. Matsuzaki M, Honkura N, Ellis-Davies GC, Kasai H. Structural basis of long-term potentiation in single dendritic spines. Nature. 2004; 429:761–766. [PubMed: 15190253]
8. Steen RG, Hamer RM, Lieberman JA. Measurement of brain metabolites by 1H magnetic resonance spectroscopy in patients with schizophrenia: a systematic review and meta-analysis. Neuropsychopharmacology. 2005; 30:1949–1962. [PubMed: 16123764]
9. Pilowsky LS, et al. First in vivo evidence of an NMDA receptor deficit in medication-free schizophrenic patients. Mol Psychiatry. 2006; 11:118–119. [PubMed: 16189506]
10. Mirnics K, Middleton FA, Lewis DA, Levitt P. Analysis of complex brain disorders with gene expression microarrays: schizophrenia as a disease of the synapse. Trends Neurosci. 2001; 24:479–486. [PubMed: 11476888]
11. Hill JJ, Hashimoto T, Lewis DA. Molecular mechanisms contributing to dendritic spine alterations in the prefrontal cortex of subjects with schizophrenia. Mol Psychiatry. 2006; 11:557–566. [PubMed: 16402129]
12. Fischer M, Kaech S, Knutti D, Matus A. Rapid actin-based plasticity in dendritic spines. Neuron. 1998; 20:847–854. [PubMed: 9620690]
13. Carlisle HJ, Kennedy MB. Spine architecture and synaptic plasticity. Trends Neurosci. 2005; 28:182–187. [PubMed: 15808352]
14. Harrison PJ, West VA. Six degrees of separation: on the prior probability that schizophrenia susceptibility genes converge on synapses, glutamate and NMDA receptors. Mol Psychiatry. 2006; 11:981–983. [PubMed: 17063182]
15. Hashimoto, R.; Tankou, S.; Takeda, M.; Sawa, A. Drugs Today. Vol. 43. Barc: 2007. Postsynaptic density: A key convergent site for schizophrenia susceptibility factors and possible target for drug development; p. 645-654.
16. Sheng M, Hoogenraad CC. The postsynaptic architecture of excitatory synapses: a more quantitative view. Annu Rev Biochem. 2007; 76:823–847. [PubMed: 17243894]
17. Blanpied TA, Kerr JM, Ehlers MD. Structural plasticity with preserved topology in the postsynaptic protein network. Proc Natl Acad Sci USA. 2008; 105:12587–12592. [PubMed: 18723686]
18. St Clair D, et al. Association within a family of a balanced autosomal translocation with major mental illness. Lancet. 1990; 336:13–16. [PubMed: 1973210]
19. Callicott JH, et al. Variation in DISC1 affects hippocampal structure and function and increases risk for schizophrenia. Proc Natl Acad Sci USA. 2005; 102:8627–8632. [PubMed: 15939883]
20. Cannon TD, et al. Association of DISC1/TRAX haplotypes with schizophrenia, reduced prefrontal gray matter, and impaired short- and long-term memory. Arch Gen Psychiatry. 2005; 62:1205–1213. [PubMed: 16275808]
21. Ishizuka K, Paek M, Kamiya A, Sawa A. A review of Disrupted-In-Schizophrenia-1 (DISC1): neurodevelopment, cognition, and mental conditions. Biol Psychiatry. 2006; 59:1189–1197. [PubMed: 16797264]
22. Chubb JE, Bradshaw NJ, Soares DC, Porteous DJ, Millar JK. The DISC locus in psychiatric illness. Mol Psychiatry. 2008; 13:36–64. [PubMed: 17912248]
23. Kirkpatrick B, et al. DISC1 immunoreactivity at the light and ultrastructural level in the human neocortex. J Comp Neurol. 2006; 497:436–450. [PubMed: 16736468]
24. Kvajo M, et al. A mutation in mouse Disc1 that models a schizophrenia risk allele leads to specific alterations in neuronal architecture and cognition. Proc Natl Acad Sci USA. 2008; 105:7076–7081. [PubMed: 18458327]
25. Kamiya A, et al. A schizophrenia-associated mutation of DISC1 perturbs cerebral cortex development. Nat Cell Biol. 2005; 7:1167–1178. [PubMed: 16299498]
26. Shi SH, et al. Rapid spine delivery and redistribution of AMPA receptors after synaptic NMDA receptor activation. Science. 1999; 284:1811–1816. [PubMed: 10364548]

27. Xie Z, et al. Kalirin-7 controls activity-dependent structural and functional plasticity of dendritic spines. Neuron. 2007; 56:640–656. [PubMed: 18031682]
28. Ma XM, Wang Y, Ferraro F, Mains RE, Eipper BA. Kalirin-7 is an essential component of both shaft and spine excitatory synapses in hippocampal interneurons. J Neurosci. 2008; 28:711–724. [PubMed: 18199770]
29. Cahill M, et al. Kalirin regulates cortical spine morphogenesis and disease-related behavioral phenotypes. Proc Natl Acad Sci USA. 2009 In press.
30. Saneyoshi T, et al. Activity-dependent synaptogenesis: regulation by a CaM-kinase kinase/CaM-kinase I/betaPIX signaling complex. Neuron. 2008; 57:94–107. [PubMed: 18184567]
31. Tolias KF, et al. The Rac1-GEF Tiam1 couples the NMDA receptor to the activity-dependent development of dendritic arbors and spines. Neuron. 2005; 45:525–538. [PubMed: 15721239]
32. Bolger GB, et al. Scanning peptide array analyses identify overlapping binding sites for the signalling scaffold proteins, beta-arrestin and RACK1, in cAMP-specific phosphodiesterase PDE4D5. Biochem J. 2006; 398:23–36. [PubMed: 16689683]
33. Millar JK, et al. DISC1 and PDE4B are interacting genetic factors in schizophrenia that regulate cAMP signaling. Science. 2005; 310:1187–1191. [PubMed: 16293762]
34. Murdoch H, et al. Isoform-selective susceptibility of DISC1/phosphodiesterase-4 complexes to dissociation by elevated intracellular cAMP levels. J Neurosci. 2007; 27:9513–9524. [PubMed: 17728464]
35. Taya S, et al. DISC1 regulates the transport of the NUDEL/LIS1/14-3-3epsilon complex through kinesin-1. J Neurosci. 2007; 27:15–26. [PubMed: 17202468]
36. Steward O, Worley PF. Selective targeting of newly synthesized Arc mRNA to active synapses requires NMDA receptor activation. Neuron. 2001; 30:227–240. [PubMed: 11343657]
37. Hsueh YP, Kim E, Sheng M. Disulfide-linked head-to-head multimerization in the mechanism of ion channel clustering by PSD-95. Neuron. 1997; 18:803–814. [PubMed: 9182804]
38. Djinovic-Carugo K, Gautel M, Ylanne J, Young P. The spectrin repeat: a structural platform for cytoskeletal protein assemblies. FEBS Lett. 2002; 513:119–123. [PubMed: 11911890]
39. Rabiner CA, Mains RE, Eipper BA. Kalirin: a dual Rho guanine nucleotide exchange factor that is so much more than the sum of its many parts. Neuroscientist. 2005; 11:148–160. [PubMed: 15746383]
40. Luo L, et al. Differential effects of the Rac GTPase on Purkinje cell axons and dendritic trunks and spines. Nature. 1996; 379:837–840. [PubMed: 8587609]
41. Tashiro A, Minden A, Yuste R. Regulation of dendritic spine morphology by the rho family of small GTPases: antagonistic roles of Rac and Rho. Cereb Cortex. 2000; 10:927–938. [PubMed: 11007543]
42. Camargo LM, et al. Disrupted in Schizophrenia 1 Interactome: evidence for the close connectivity of risk genes and a potential synaptic basis for schizophrenia. Mol Psychiatry. 2007; 12:74–86. [PubMed: 17043677]
43. Ishizuka K, et al. Evidence that many of the DISC1 isoforms in C57BL/6J mice are also expressed in 129S6/SvEv mice. Mol Psychiatry. 2007; 12:897–899. [PubMed: 17895924]
44. Jaaro-Peled H, et al. Neurodevelopmental mechanisms of schizophrenia: understanding disturbed postnatal brain maturation through Neuregulin-1 and DISC1. Trends Neurosci. 2009; 32:485–95. [PubMed: 19712980]
45. McGlashan TH, Hoffman RE. Schizophrenia as a disorder of developmentally reduced synaptic connectivity. Arch Gen Psychiatry. 2000; 57:637–648. [PubMed: 10891034]
46. Schurov IL, Handford EJ, Brandon NJ, Whiting PJ. Expression of disrupted in schizophrenia 1 (DISC1) protein in the adult and developing mouse brain indicates its role in neurodevelopment. Mol Psychiatry. 2004; 9:1100–1110. [PubMed: 15381924]
47. Holtmaat AJ, et al. Transient and persistent dendritic spines in the neocortex in vivo. Neuron. 2005; 45:279–291. [PubMed: 15664179]
48. McGlashan TH, Johannessen JO. Early detection and intervention with schizophrenia: rationale. Schizophr Bull. 1996; 22:201–222. [PubMed: 8782282]

49. Koike H, Arguello PA, Kvajo M, Karayiorgou M, Gogos JA. Disc1 is mutated in the 129S6/SvEv strain and modulates working memory in mice. Proc Natl Acad Sci USA. 2006; 103:3693–3697. [PubMed: 16484369]

50. Cai X, Gu Z, Zhong P, Ren Y, Yan Z. Serotonin 5-HT1A receptors regulate AMPA receptor channels through inhibiting Ca2+/calmodulin-dependent kinase II in prefrontal cortical pyramidal neurons. J Biol Chem.

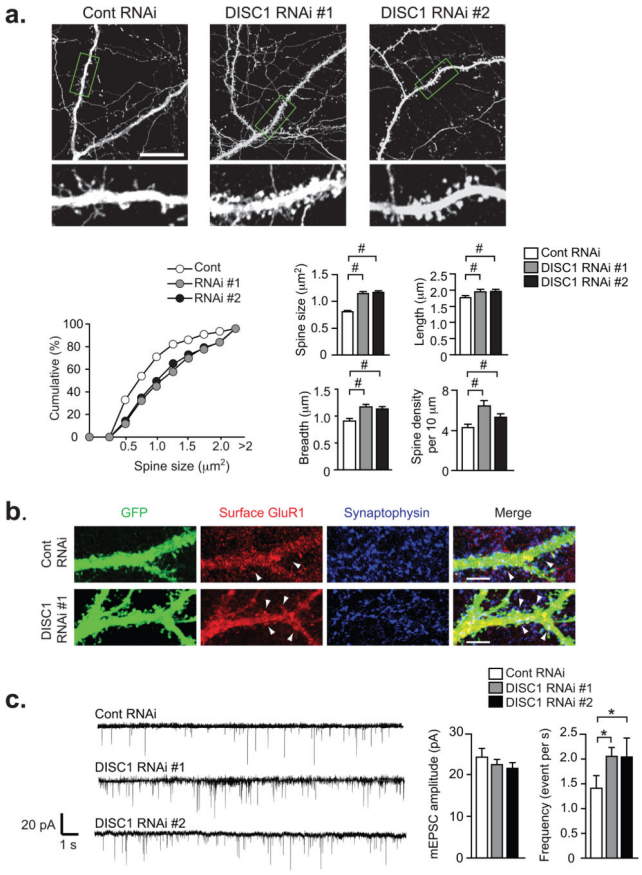


**Figure 1. Short-term knockdown of DISC1 elicits spine enlargement in rat primary cortical neurons**

(**a**) Spine changes in mature neurons by short-term knockdown (2 days) of DISC1 with use of two independent RNAi against DISC1. Scale bar, 50 μm. (**b**) Enhanced surface expression of GluR1 on the spine, Arrowheads, GluR1 clustering on spines. (**c**) Increase in the frequency of miniature excitatory postsynaptic currents (mEPSC). Left, representative mEPSC traces; right, mEPSC amplitude and frequency. Bar, s.e.m. **P* < 0.05, #*P* < 0.001.

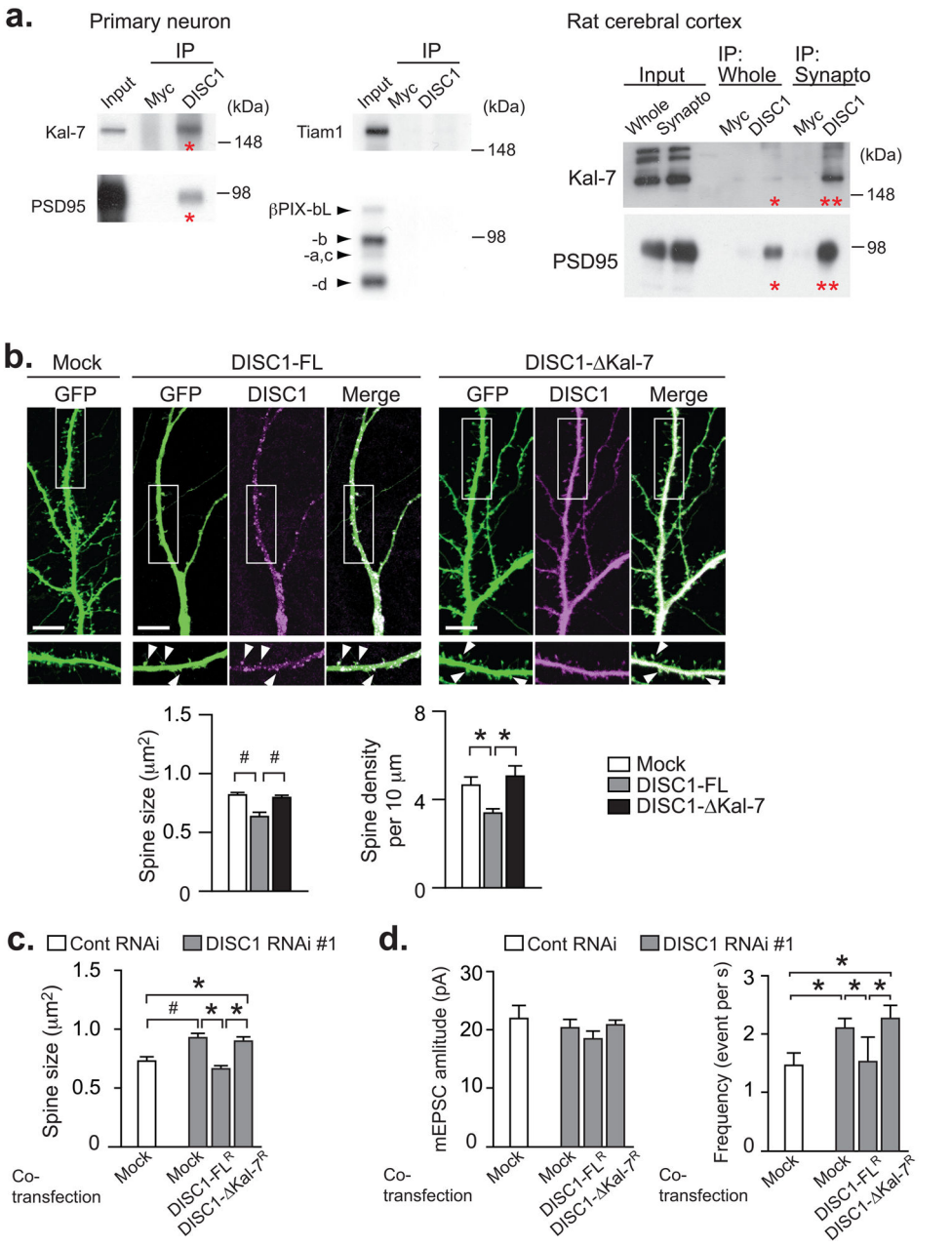


**Figure 2. Protein interaction of DISC1/Kal-7 regulates spine morphology in rat primary cortical neurons**

(**a**) Endogenous interactions of DISC1 with Kal-7 and PSD95 (red asterisks) by co-immunoprecipitation (IP) from primary cortical neurons and rat cerebral cortex. DISC1 did not bind Tiam1 norβPIX. Strong interactions of DISC1/Kal-7 and DISC1/PSD95 are observed in the synaptosomal fractions (double asterisks). Full-length blots are presented in Supplementary Fig. 17. (**b**) Spine shrinkage and reduced spine density by overexpression (for 2 days) of full length DISC1 (DISC-FL), but not by DISC1 lacking Kal-7 interaction (DISC1-ΔKal-7). Both DISC1-FL and DISC1-ΔKal-7 were localized in the dendritic spine (arrowheads). (**c**) Normalization of DISC1 knockdown-induced spine enlargement by

DISC1-FL, but not by DISC1-ΔKal-7. (**d**) Increase in the frequency of mEPSC was normalized by the overexpression of DISC1-FL$^{R}$, but not by that of DISC1-ΔKal-7$^{R}$. Left, representative mEPSC traces; right, mEPSC amplitude and frequency. Bar, s.e.m. *$P < 0.05$, #$P < 0.001$.

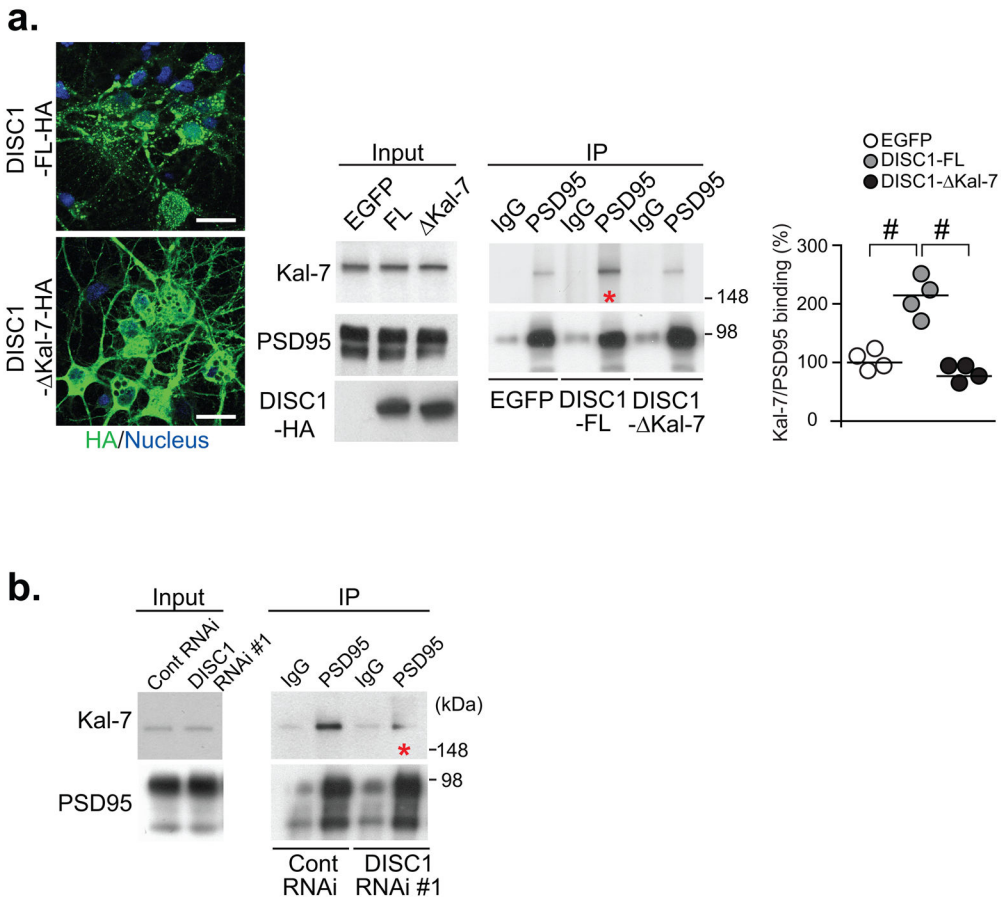


**Figure 3. Augmentation of Kal-7/PSD95 protein binding by DISC1 in rat primary cortical neurons**

(**a**) Increased Kal-7/PSD95 protein binding by overexpression of DISC1. Left, immunofluorescent cell staining indicating that majority of neurons are infected with Sindbis virus expressing DISC1-FL-HA or DISC1-ΔKal-7-HA. Middle and right, increased binding of Kal-7 and PSD95 by overexpression of DISC1-FL (asterisk), but not DISC1-ΔKal-7. Scale bar, 20 μm. (**b**) Decrease in Kal-7/PSD95 binding upon lentivirus-based DISC1 knockdown. *$P < 0.05$, #$P < 0.001$. Full-length blots are presented in Supplementary Fig. 17.

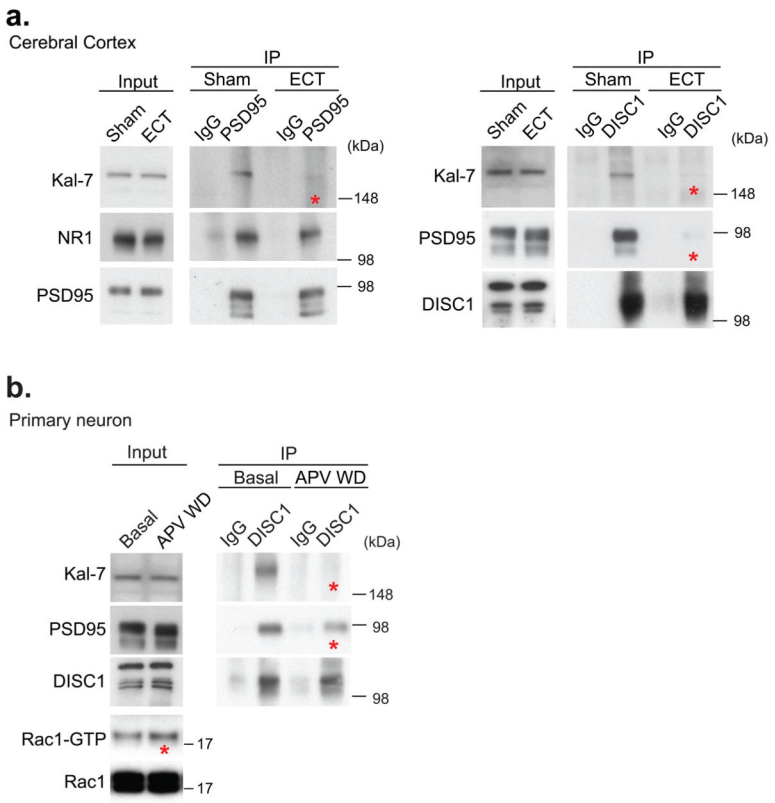


**Figure 4. Protein interaction of DISC1/Kal-7/PSD95 influenced by activation of the NMDA-type glutamate receptor**

(**a**) Decrease in interactions among DISC1, Kal-7, and PSD95 (asterisks) three min after electroconvulsive treatment (ECT) in rat brains *in vivo*. Full-length blots are presented in Supplementary Fig. 18. (**b**) Decrease in interactions of DISC1/Kal-7 and DISC1/PSD95 (asterisk) as well as activation of Rac1 (input, asterisk) after selective activation of the NMDA receptor by APV withdrawal (WD). **P* < 0.05. Full-length blots are presented in Supplementary Fig. 18.

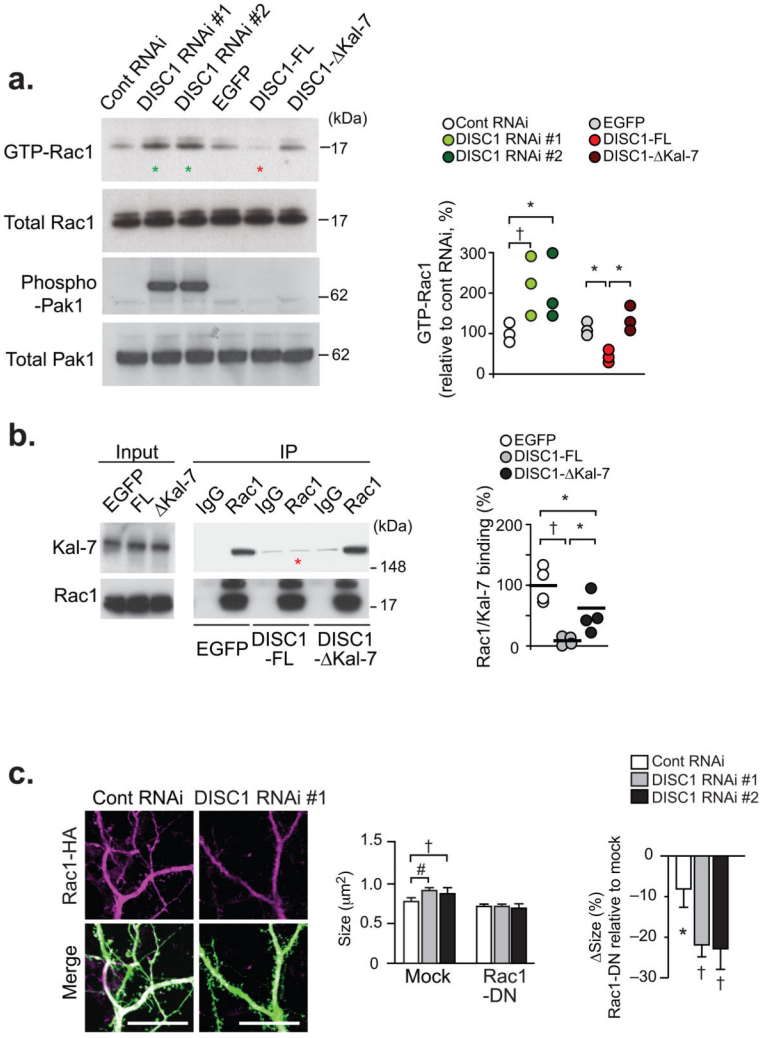


**Figure 5. Regulation of Rac1 activity via "signalosome" of DISC1/Kal-7**

(**a**) Inhibition of Rac1 activity (level of GTP-Rac1) by DISC1-FL (red asterisk), but not DISC1-ΔKal-7, and augmentation of the activity by DISC1 knockdown (green asterisk) in primary cortical neurons. Augmented Rac1 activity is also monitored by phosphorylation of Pak1. Full-length blots are presented in Supplementary Fig. 18. (**b**) Decreased Rac1/Kal-7 binding by DISC1-FL (red asterisk), not by DISC1-ΔKal-7. (**c**) Key role of Rac1 in DISC1-regulated spine enlargement, as evident by its blockade by expression of Rac1-DN (dominant-negative). Scale bar, 20 μm. Bar, s.e.m. Significant effects of Rac1-DN compared to mock are shown as $*P < 0.05$, †$P < 0.01$, #$P < 0.001$. Full-length blots are presented in Supplementary Fig. 18.

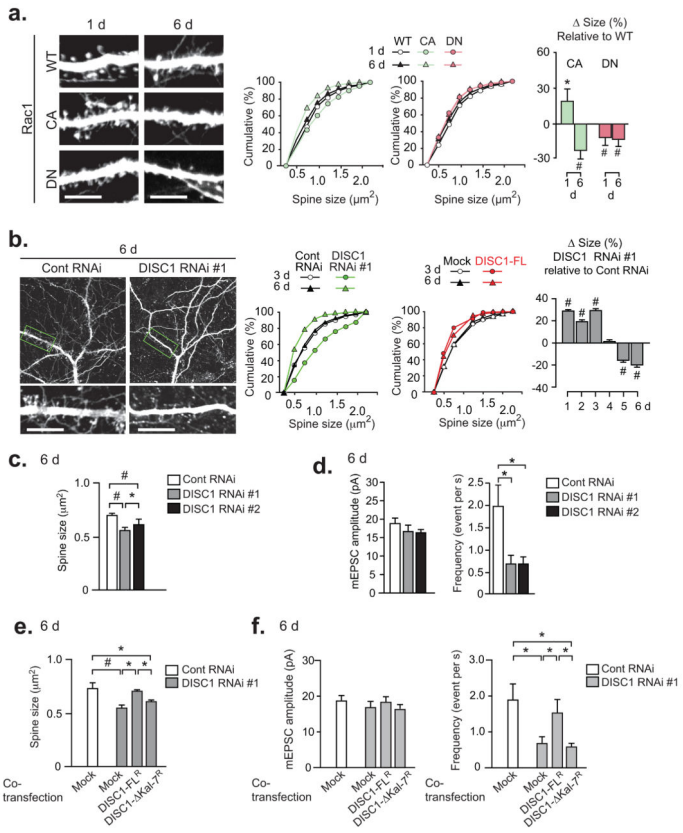


**Figure 6. Long-term disturbance of DISC expression leads to spine shrinkage in rat primary cortical neurons**

(**a**) Short- or long-term effect of Rac1 [WT (wild-type), CA (constitutively-active), or DN] on spine morphology in mature neurons. Bars, -fold changes of spine size by introduction with Rac1-CA or -DN relative to that with Rac1-WT. (**b**) Short- or long-term effect of DISC1 knockdown (in green) or overexpression (in red) in mature neurons. (**c**) Reduced spine size by knockdown of DISC1 for 6 days in primary cortical culture. (**d**) Decrease in mEPSC by long-term DISC1 knockdown. (**e**) Spine deterioration (decreased spine size) by long-term knockdown of DISC1 was normalized by overexpression of DISC1-FL, but not by that of DISC1-ΔKal-7. **P* < 0.05, #*P* < 0.001. **(f**) Spine deterioration (decreased mEPSC frequency) by long-term knockdown of DISC1 was normalized by overexpression of DISC1-FL, but not by that of DISC1-ΔKal-7. Bar, s.e.m. **P* < 0.05. Scale bar, 10 μm.

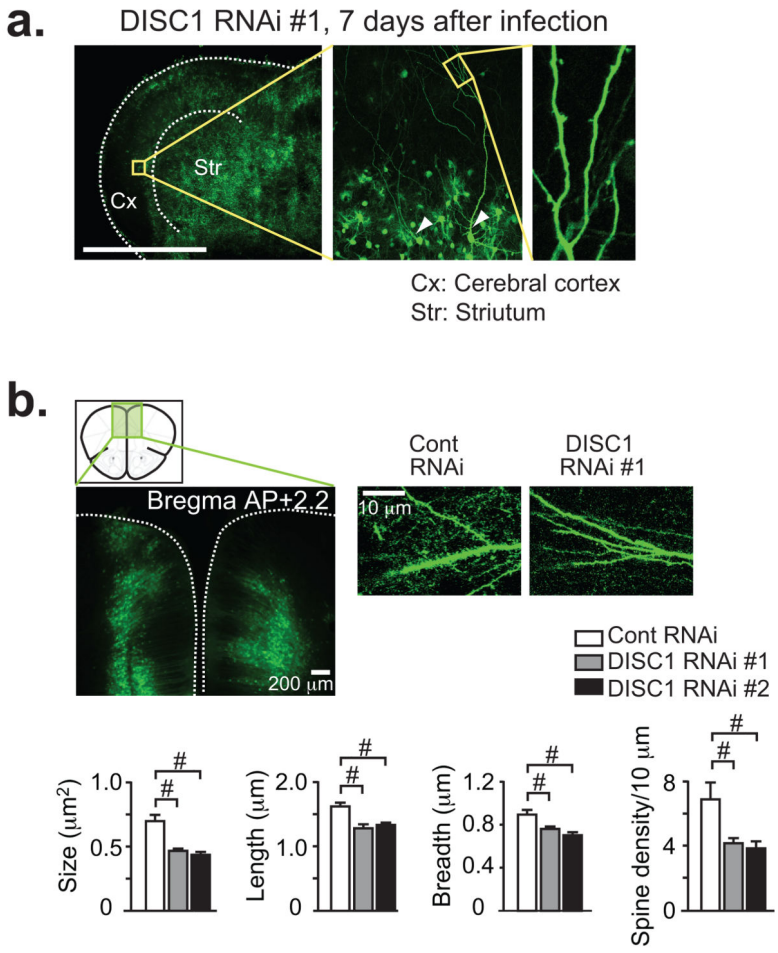


**Figure 7. Long-term suppression of DISC1 leads to spine shrinkage in slices and brains *in vivo***

(**a**) Effect of long-term DISC1 knockdown on spine morphology in rat organotypic cortical culture. Representative image of culture with DISC1 RNAi (green). Scale bar, 5 mm. (**b**) Long-term effect of DISC1 knockdown on spine size in the medial prefrontal cortex. Bar, s.e.m. #$P < 0.001$.